



In vitro and *in vivo* metabolic tagging and modulation of platelets

Dhyanesh Baskaran^a, Yusheng Liu^a, Jiadiao Zhou^a, Yueji Wang^a, Daniel Nguyen^a, Hua Wang^{a,b,c,d,e,f,g,h,*}

^a Department of Materials Science and Engineering, University of Illinois at Urbana-Champaign, Urbana, IL, 61801, USA

^b Cancer Center at Illinois (CCIL), Urbana, IL, 61801, USA

^c Institute for Genomic Biology, University of Illinois at Urbana-Champaign, Urbana, IL, 61801, USA

^d Department of Bioengineering, University of Illinois at Urbana-Champaign, Urbana, IL, 61801, USA

^e Carle College of Medicine, University of Illinois at Urbana-Champaign, Urbana, IL, 61801, USA

^f Beckman Institute for Advanced Science and Technology, University of Illinois at Urbana-Champaign, Urbana, IL, 61801, USA

^g Materials Research Laboratory, University of Illinois at Urbana-Champaign, Urbana, IL, 61801, USA

^h Grainger College of Engineering, University of Illinois at Urbana-Champaign, Urbana, IL, 61801, USA

ARTICLE INFO

Keywords:

platelet
Metabolic glycan labeling
Sugar
Click chemistry
Cell engineering

ABSTRACT

Platelets play a critical role in hemostasis at sites of injury and are capable of interacting with various types of cells in the bloodstream. The promise of utilizing platelets for diagnostic and therapeutic applications has motivated the development of facile strategies to functionalize platelets. However, platelets with a small size, lack of nucleus and efficient protein machinery, and low tolerance to chemicals and transfection agents have posed significant challenges for chemical or genetic engineering. Here, for the first time, we report successful metabolic glycan labeling of platelets to introduce chemical tags (e.g., azido groups) onto the membrane of platelets. We demonstrate that azido-sugars can metabolically label platelets in a concentration dependent manner, with cell-surface azido groups detectable at as early as 4 hours. The cell-surface azido groups enable the conjugation of various macromolecular cargos including proteins and polymers onto platelets via efficient click chemistry. Small-molecule drugs such as doxorubicin can also be conjugated onto azido-labeled platelets and become subsequently released to kill surrounding cancer cells, demonstrating the feasibility of utilizing platelets as a drug delivery vehicle. We further show that azido-sugars, upon intraperitoneal injection, can metabolically label platelets with azido groups *in vivo*, which persist for up to 4 days in mice (nearly the life-span of murine platelets). This *in vitro* and *in vivo* platelet labeling and targeting technology opens a new avenue to platelet-based diagnostics and therapeutics.

1. Introduction

Platelets are small anucleate cells that circulate in the bloodstream and make up ~1 % of whole blood. They are short-lived with a lifespan of 4–5 days in mice and 7–10 days in humans [1,2]. Platelets play a critical role in hemostasis at sites of injury or surgery [3,4]. Upon bleeding, platelets are rapidly recruited to initiate the formation of blood clots [5] and gradually release adenosine diphosphate (ADP), thromboxane A2 and other activation factors to further recruit platelets and immune cells to promote hemostasis and initiate tissue restoration [6–8]. Platelets are also involved in innate immunity by directly binding to bacteria and viruses [9–11]. Cancer cells were also reported to interact with platelets, and the transfer of PD-L1 from cancer cells to

platelets has been explored for cancer prognosis [11,12]. The ability to home to injury sites, recruit immune cells, and interact with various types of cells makes platelets an attractive target for diagnostic and therapeutic applications, which poses a demand for effective and facile strategies to engineer platelets.

Existing platelet engineering methods can be divided into genetic and chemical conjugation approaches [13]. Megakaryocytes and other platelet precursor cells can be genetically engineered *ex vivo*, followed by infusion or transplantation to the bone marrow to produce genetically engineered platelets [14–17]. Anucleate platelets can also be transfected with mRNA-encapsulating lipid nanoparticles to express exogenous proteins [18–22]. However, the complexity and safety concerns of genetic engineering methods remain to be resolved. Direct

* Corresponding author. Department of Materials Science and Engineering, University of Illinois at Urbana-Champaign, Urbana, IL 61801, USA.

E-mail address: huawang3@illinois.edu (H. Wang).

chemical conjugation of cargos to platelets has been explored by treating platelets with the Traut's reagent and then conjugating with disulfide-bearing molecules. For example, anti-PD-1 was conjugated to platelets via Traut's reagent for the delivery of anti-PD-1 to the tumor site where platelets tend to accumulate [23,24]. Cargos can also be conjugated to platelets by installing a targeting moiety that can bind to surface receptors of platelets such as platelet integrin GPIIb/IIIa [25–27]. These chemical approaches, though, have only been successful for *in vitro* engineering of platelets to date. The use of the Traut's agent and antibodies was also shown to lead to the activation of platelets prior to transfusion and thus result in a higher chance of thrombosis during

platelet infusion [25,28,29].

Here we report a facile platelet engineering approach via the metabolic glycoengineering processes of unnatural sugars. We show that anucleate platelets can take up and metabolize azido-sugars (e.g., tetraacetyl-*N*-azidoacetyl mannosamine (Ac_4ManAz)), leading to the expression of azido-labeled glycoproteins on platelets (Fig. 1a) [30–33]. The cell-surface azido groups can be detected as early as 4 h post azido-sugar incubation, and the density of cell-surface azido groups increases with the concentration and incubation time of azido-sugars. Intraperitoneally administered azido-sugars also successfully labeled mouse platelets in the bloodstream with azido groups, and the surface

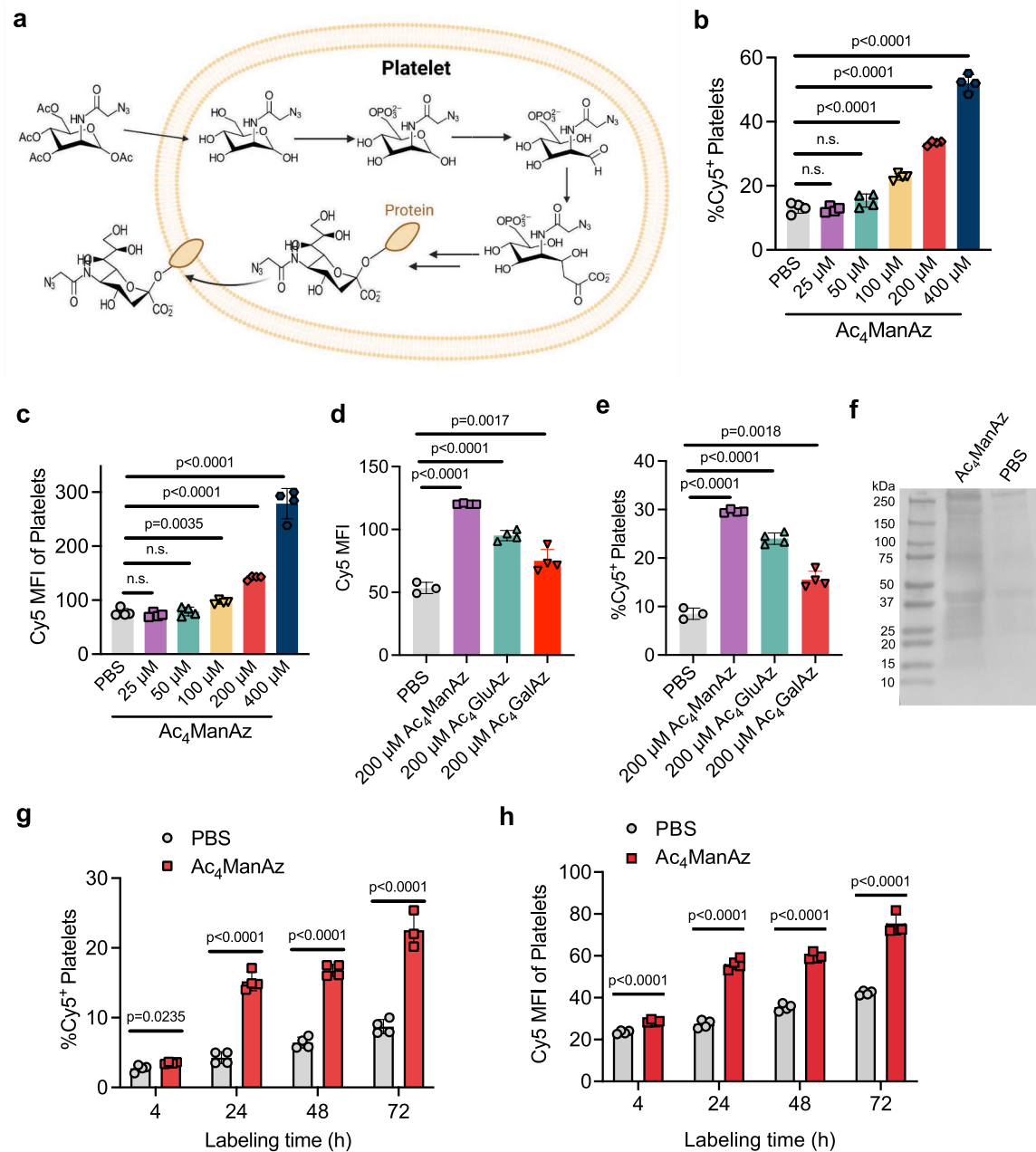


Fig. 1. *In vitro* metabolic glycan labeling of primary platelets. (a) Schematic illustration of metabolic glycan labeling of platelets by azido-sugars. (b) % $\text{Cy}5^+$ platelets and (c) mean $\text{Cy}5$ fluorescence intensity of platelets after 4-h incubation with Ac_4ManAz and staining with DBCO-Cy5 ($n = 4$). (d) % $\text{Cy}5^+$ platelets and (e) mean $\text{Cy}5$ fluorescence intensity of platelets after 4-h incubation with 200 μM Ac_4ManAz , Ac_4GluAz , or Ac_4GalAz , and staining with DBCO-Cy5 ($n = 4$). (f) Western blot analysis of azido-labeled glycoproteins in platelets. Azido-proteins were converted to biotinylated ones and then detected via streptavidin-HRP. (g) % $\text{Cy}5^+$ platelets and (h) mean $\text{Cy}5$ fluorescence intensity of platelets after incubation with 100 μM Ac_4ManAz for different times ($n = 4$). Cells were stained with DBCO-Cy5 prior to flow cytometry analysis. All the numerical data are presented as mean \pm SD (one-way ANOVA with post hoc Tukey's LSD test was used for (b–e) or two tailed unpaired student's t-test was used for (g,h); n.s., $P > 0.05$; $0.01 < P \leq 0.05$; $^{**}P \leq 0.01$; $^{***}P \leq 0.001$; $^{****}P \leq 0.0001$).

azido groups could persist for up to 4 days *in vivo*, nearly the lifespan of mouse platelets. We also demonstrate that azido-labeled platelets enable conjugation of dibenzocyclooctyne (DBCO)-bearing macromolecular and small-molecule cargos via efficient click chemistry [34,35]. Small-molecule doxorubicin, after conjugation onto platelets, can also be gradually released to kill surrounding cancer cells. The metabolic labeling approach did not induce any noticeable toxicity to platelets. This facile platelet engineering approach could greatly facilitate the development of platelet-based therapeutics and diagnostics and provides a new avenue to probing the interaction between platelets and other types of cells.

2. Results and discussion

2.1. *In vitro* metabolic glycan labeling of platelets

We first studied the metabolic glycan labeling of platelets *in vitro*. Platelets were isolated from the blood of C57BL/6 mice via a series of centrifugation steps and resuspended in a Modified Tyrode's Calcium Free Buffer supplemented with Prostaglandin E-1 (Fig. S1), followed by the addition of different concentrations of Ac₄ManAz or PBS. After 4 h, platelets were stained with DBCO-Cy5 to detect cell-surface azido groups (Fig. S2). Compared to cells treated with PBS, platelets treated with 100 μM Ac₄ManAz showed significantly higher Cy5 fluorescence intensity, indicating the successful labeling of platelets with azido groups (Fig. 1b–c). By increasing the concentration of Ac₄ManAz from 100 μM to 400 μM, the labeling efficiency of platelets was further increased (Fig. 1b–c). We also compared the metabolic labeling efficiency of different types of azido-sugars, i.e. Ac₄ManAz, tetraacetyl-*N*-azidoacetyl glucosamine (Ac₄GluAz) and tetraacetyl-*N*-azidoacetyl galactosamine (Ac₄GalAz) (Fig. 1d–e). Compared to Ac₄GluAz and Ac₄GalAz, Ac₄ManAz showed a significantly higher labeling efficiency for platelets (Fig. 1d–e). To confirm the azido labeling of glycoproteins in platelets, we isolated proteins from Ac₄ManAz- or PBS-treated platelets and performed the western blot analysis by converting azido-proteins to biotinylated ones and detecting them with HRP-streptavidin and chemiluminescence imaging. Compared to the PBS group, Ac₄ManAz group showed a significantly higher signal for multiple protein bands, confirming the successful azido labeling of glycoproteins (Fig. 1f).

As we intended to study the metabolic labeling efficiency of platelets for an extended time, we first optimized the culture media for platelets by comparing the viability of platelets in different buffers at varied incubation temperature (4°C, 25°C, or 37°C). Three buffers were tested: Alsever's solution (ALS) supplemented with bovine serum albumin (BSA), Modified Tyrode's Calcium free Buffers with high NaHCO₃ (PB1) [26], and Modified Tyrode's Calcium free Buffers with low NaHCO₃ (PB2) [27]. The viability of platelets was higher at 4°C and 25°C than at 37°C across all the buffers (Figs. S3a–c). In general, PB2 resulted in a higher viability and CD41 (a well-known surface marker of platelets) expression level of platelets than ALS or PB1 (Figs. S3a–c). The best platelet culture method that we observed was to culture platelets in PB2 at 25°C, as cold stored platelets were reported to exhibit altered morphology and faster clearance after infusion [36–38]. After optimizing the cell media and culturing conditions, we were able to store primary platelets for up to 3 days. By increasing incubation time of platelets with Ac₄ManAz from 4 h to 24 h, the azido labeling efficiency was dramatically enhanced (Fig. 1g–h). By further increasing the Ac₄ManAz treatment time from 24 h to 48 h or 72 h, the labeling efficiency was slightly enhanced (Fig. 1g–h). It is noteworthy that 24-h incubation with Ac₄ManAz did not induce any noticeable changes in the morphology of platelets in comparison with the PBS group (Figs. S4a–b).

2.2. Membrane retention of cell-surface azido groups

We next studied the stability of cell-surface azido groups on platelets. Platelets were incubated with 100 μM Ac₄ManAz or PBS for 24 h, and then transferred to Ac₄ManAz-free fresh media. At 6 h post the media change, Ac₄ManAz-treated platelets still exhibited a decent azido density on the cell surface (Fig. 2a–b). At 12 h, Cy5 fluorescence intensity of Ac₄ManAz- and PBS-treated platelets after DBCO-Cy5 staining showed negligible differences (Fig. 2a–b), indicating the decay of azido density on the surface of platelets. It is noteworthy that the treatment of platelets with Ac₄ManAz did not induce any decrease in platelet viability compared to PBS treatment (Fig. 2c). This is supported by the mitochondria potential assay, which showed negligible differences in the vitality of mitochondria between Ac₄ManAz and PBS groups (Fig. S5a). We also incubated platelets with Ac₄ManAz or PBS for 24 h, 48 h, and 72 h, respectively, and stained them with Annexin-APC and Calcein AM to detect the necrotic population (Annexin⁺Calcein AM[−]). As a result, negligible differences in the fraction of necrotic cells were detected between Ac₄ManAz and PBS groups (Fig. S5b). To study whether Ac₄ManAz treatment has any effect on the activation status of platelets, we analyzed the surface expression of CD62p, an activation marker of platelets, via flow cytometry. At 12 h, Ac₄ManAz treatment did not induce any noticeable change on CD62p expression levels of platelets in comparison with PBS treatment (Fig. 2d). At 24 or 48 h, Ac₄ManAz-treated platelets showed reduced CD62p expression in comparison with PBS-treated platelets, indicating the lower activation status of platelets at later times (Fig. 2d). We also performed a clotting assay using collagen-coated glass slides. 2.5 mM Ca²⁺ was added to the platelet media and then platelets were added onto collagen-coated or non-coated glass slides. As a result, platelets pretreated with PBS or Ac₄ManAz for 24 h both formed aggregates in 10 min on the collagen-coated glass slide (Fig. S6). These data demonstrated that 24-h treatment with Ac₄ManAz does not induce the necrosis of platelets or impair the coagulation capabilities and vitality of platelets.

2.3. Conjugation of macromolecular cargos to platelets

We next explored the conjugation of cargos, especially macromolecular cargos, onto azido-labeled platelets via efficient click chemistry (Fig. 3a). Allophycocyanin (APC), a fluorescent protein with a molecular weight of 105 KDa, was modified with DBCO via amine-*N*-hydroxysuccinimide chemistry (Fig. S7a). UV-vis spectrometry confirmed the successful modification of APC with DBCO (Fig. S7b). After treating platelets with Ac₄ManAz or PBS for 24 h and then incubating them with DBCO-APC, a significantly higher APC fluorescence intensity was detected on Ac₄ManAz-treated platelets than PBS-treated platelets (Fig. 3b–d). Confocal imaging also showed the overlay of APC and CD41 (Fig. 3b, Fig. S8), confirming the successful conjugation of DBCO-APC to azido-labeled platelets. By staining cells with biotin-conjugated anti-APC and FITC-avidin, we monitored the retention of conjugated APC on platelets. As a result, the conjugated APC was still detectable on the surface of platelets at 12 h post DBCO-APC conjugation (Fig. S9). Phycoerythrin (PE), another fluorescent protein with a molecular weight of 240 KDa, can also be modified with DBCO using the amine-*N*-hydroxysuccinimide chemistry (Fig. S10). Similarly, Ac₄ManAz-treated platelets could capture more DBCO-PE than PBS-treated platelets (Fig. 3e–f), indicating the successful conjugation of DBCO-PE to azido-labeled platelets. We also synthesized DBCO-functionalized polyacrylic acid (PAA), which was confirmed via ¹H NMR spectrometry (Fig. S11). DBCO-PAA, with a much lower cell uptake background, showed a significant targeting effect towards azido-labeled platelets, in comparison with unlabeled platelets (Fig. 3g–h).

2.4. Surface conjugation and release of doxorubicin

As platelets naturally home to sites of injury or inflammation, they

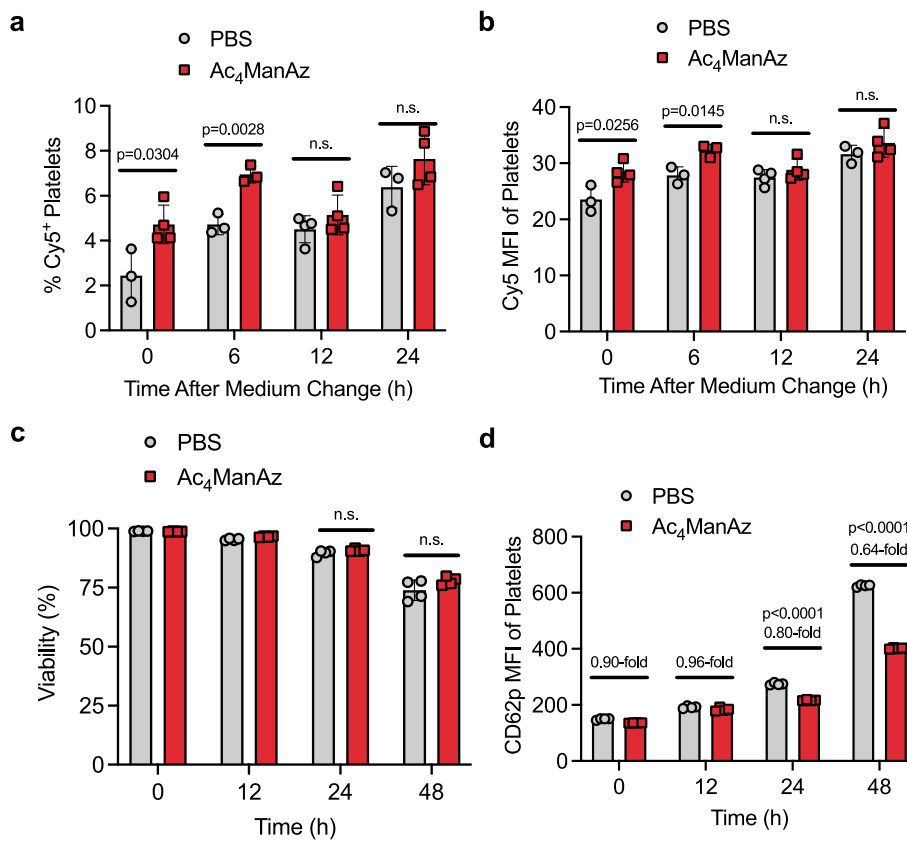


Fig. 2. Azido-glycans can retain on platelets for over 6 h *in vitro* without noticeable cytotoxicity towards platelets. (a-b) Platelets were incubated with 100 μ M Ac₄ManAz for 24 h, and further incubated in fresh media for different times. At each time point, platelets were stained with DBCO-Cy5 and analyzed via flow cytometry. Shown are (a) % Cy5⁺ platelets and (b) mean Cy5 fluorescence intensity of platelets at different times ($n = 4$). (c) Viability of platelets in the presence or absence of Ac₄ManAz for 0, 12, 24, and 48 h, respectively ($n = 4$). (d) CD62p expression levels of platelets incubated with 100 μ M Ac₄ManAz or PBS for 0, 12, 24, and 48 h, respectively ($n = 4$). All the numerical data are presented as mean \pm SD (two tailed unpaired student's t-test was used; n.s., $P > 0.05$; $0.01 < *P \leq 0.05$; $**P \leq 0.01$; $***P \leq 0.001$; $****P \leq 0.0001$).

have been actively explored as drug carriers for the treatment of cancer and other diseases. As a proof-of-concept demonstration, we tested the feasibility of conjugating DBCO-doxorubicin onto azido-labeled platelets for subsequent release of doxorubicin to effect on neighboring cancer cells (Fig. 4a). We first synthesized DBCO-hz-Dox with an acid-labile hydrazone bond (Fig. S12). DBCO-hz-Dox exhibited a much higher degradation rate at pH 5.4 than at pH 7.4, as expected (Fig. 4b). To study the conjugation of DBCO-hz-dox to azido-labeled platelets, platelets isolated from C57BL/6 mice were treated with Ac₄ManAz or PBS for 24 h, followed by incubation with DBCO-hz-Dox for 1 h. Compared to PBS-treated platelets, Ac₄ManAz-treated platelets showed a significantly higher Dox signal (Fig. 4c-d), demonstrating the successful conjugation of DBCO-hz-Dox to Ac₄ManAz-treated platelets. Next, we studied whether Dox conjugated to platelets can be gradually released to kill neighboring cancer cells, by incubating Ac₄ManAz- or PBS-treated platelets with DBCO-hz-Dox for 30 min and then coculturing platelets with C1498 acute myeloid leukemia (AML) cells for 48 h. At a DBCO-hz-dox concentration of 100 μ M, Ac₄ManAz-treated platelets resulted in a significantly lower viability of C1498 cells than PBS-treated platelets (Fig. 4e), demonstrating the feasibility of conjugating drugs onto platelets for subsequent gradual release of drugs and cancer cell killing.

2.5. In vivo metabolic labeling of platelets

We next explored *in vivo* metabolic labeling of circulating platelets. Ac₄ManAz or PBS was intraperitoneally (i.p.) injected into C57BL/6 mice every 12 h for three days. At different times post the last injection

of Ac₄ManAz or PBS, platelets were harvested from the blood, stained with DBCO-Cy5, and analyzed via flow cytometry and confocal imaging (Fig. 5a). At 6 h, a significantly higher Cy5 fluorescence intensity was observed on platelets isolated from Ac₄ManAz-treated mice than platelets isolated from PBS-treated mice (Fig. 5b-c), indicating the successful *in vivo* metabolic labeling of platelets with azido groups by Ac₄ManAz. At 48 h, platelets from Ac₄ManAz-treated mice still showed a much higher Cy5 fluorescence intensity than those from PBS-treated mice (Fig. 5b-c). At 4 days post the injections of Ac₄ManAz, a higher Cy5⁺ platelets were still detected for Ac₄ManAz group, despite a similar mean Cy5 fluorescence intensity between Ac₄ManAz and PBS groups (Fig. 5b-c). At 6 days, platelets from Ac₄ManAz- or PBS-treated mice showed negligible differences in Cy5 signal (Fig. 5b-c), indicating the loss of azido groups on circulating platelets after 6 days. The decreased azido density from day 2 to day 4 and complete turn-over on day 6 aligns with the life-span of mouse platelets (3–5 days). Confocal imaging also confirmed the presence of azido-labeled platelets in Ac₄ManAz-treated mice on day 2 (Fig. 5d, Fig. S13). We also performed a functional assay to compare the activation status of platelets between Ac₄ManAz- and PBS-treated mice. ADP, a platelet agonist, was added to platelets in Ca²⁺-containing media, followed by flow cytometry analysis of CD62 expression levels. A negligible difference in CD62p level was observed between Ac₄ManAz-treated platelets and PBS-treated platelets (Fig. 5e-f), demonstrating the minimal effect of Ac₄ManAz treatment on the activation status of platelets *in vivo*. We also performed a tail bleed assay by amputating the tail of C57BL/6 mice, which showed negligible differences in the time of bleeding cessation for PBS- and Ac₄ManAz-treated mice (Fig. 5g).

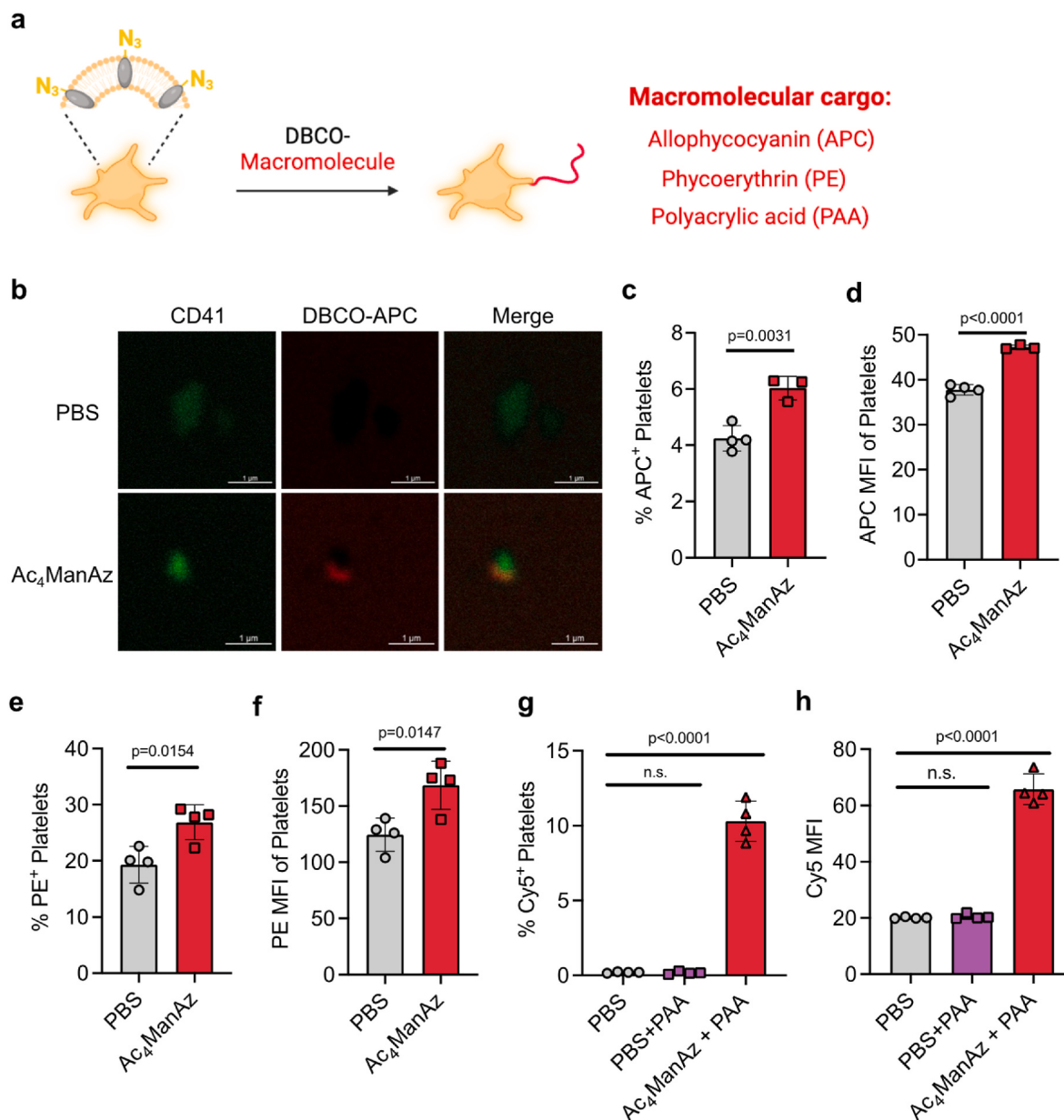


Fig. 3. Azido-labeled platelets enable conjugation of macromolecular cargos. (a) Schematic illustration of metabolic labeling of platelets and subsequent conjugation of macromolecules onto platelets. (b) Representative CLSM images of platelets that were treated with Ac₄ManAz or PBS for 24 h and then incubated with DBCO-APC for 1 h. (c) % APC⁺ platelets and (d) mean APC fluorescence intensity of platelets that were treated with Ac₄ManAz or PBS for 24 h and then incubated with DBCO-APC for 1 h ($n = 4$). (e) % PE⁺ platelets and (f) mean PE fluorescence intensity of platelets that were treated with Ac₄ManAz or PBS for 24 h and then incubated with DBCO-PE for 1 h ($n = 4$). (g) % Cy5⁺ platelets and (h) mean Cy5 fluorescence intensity of platelets that were treated with Ac₄ManAz or PBS for 24 h and then incubated with DBCO/Cy5-PAA for 1 h ($n = 4$). All the numerical data are presented as mean \pm SD (two tailed unpaired student's t-test was used for (c–f) and one-way ANOVA with post hoc Tukey's LSD test was used for (g, h); n.s., $P > 0.05$; $0.01 < *P \leq 0.05$; $**P \leq 0.01$; $***P \leq 0.001$; $****P \leq 0.0001$).

3. Discussion

Facile and efficient methods to engineer or functionalize platelets hold great promise for various diagnostic and therapeutic applications owing to the inherent injury-targeting nature of platelets. Here we present a facile strategy to modify platelet membrane with azido groups for subsequent targeted conjugation of any molecules of interest via efficient click chemistry. We demonstrated that rapid *in vitro* platelet labeling is feasible by incubating platelets with azido-sugar for only 4 h, which is critical for *ex vivo* manufacturing of short-lived platelets. To better mimic human platelet transfusion conditions, we tested the metabolic labeling of platelets for an extended time, which showed that longer incubation times (e.g., 24 h) could lead to a higher labeling

efficiency. The azido groups on the membrane of murine platelets could retain for 6–12 h post removal of azido-sugars *in vitro*. Viability and activation status tests showed negligible differences between azido-sugar-treated platelets and control platelets. These experiments demonstrated that simple incubation of platelets with azido-sugars for 4–24 h provides a facile and safe approach to tagging platelets for subsequent tracking and targeting purposes.

After demonstrating and optimizing *in vitro* metabolic labeling of platelets, we explored the targeted conjugation of DBCO-cargos to platelets via efficient click chemistry. Macromolecular APC, PE, and PAA, upon facile DBCO functionalization, can all be conjugated onto azido-labeled platelets. Small-molecule doxorubicin, with DBCO functionalization, can also be conjugated to azido-labeled platelets and then

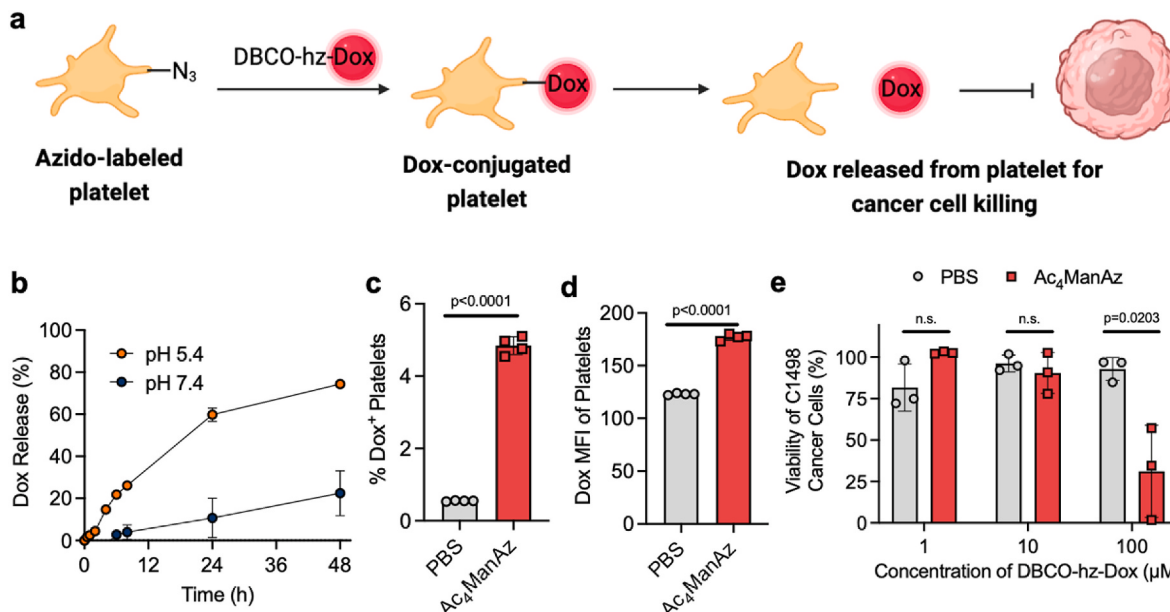


Fig. 4. Doxorubicin can be conjugated to platelets and gradually released to kill neighboring cancer cells. (a) Schematic illustration of conjugation of DBCO-hz-Dox to azido-labeled platelet and subsequent release of Dox from platelets. (b) Release kinetics of DBCO-hz-Dox at pH 7.4 and pH 5.4, respectively ($n = 3$). (c-d) Platelets pretreated with Ac₄ManAz or PBS for 24 h were incubated with 10 μ M DBCO-hz-Dox for 1 h. Shown are (c) percentages of Dox⁺ platelets and (d) mean Dox fluorescence intensity of platelets ($n = 4$). (e) Viability of C1498 AML cells after 48-h incubation with platelets ($n = 3$). Platelets were pretreated with Ac₄ManAz or PBS for 24 h and incubated with DBCO-hz-Dox (1, 10, and 100 μ M, respectively) for 1 h, following the removal of non-conjugated DBCO-hz-Dox and the coculturing with C1498 AML cells for 48 h. All the numerical data are presented as mean \pm SD (two tailed unpaired student's t-test was used; n.s., $P > 0.05$; $0.01 < *P \leq 0.05$; ** $P \leq 0.01$; *** $P \leq 0.001$; **** $P \leq 0.0001$).

become gradually released from platelets to kill surrounding AML cells, demonstrating the feasibility to utilize platelets as a targetable drug depot. *Ex vivo* metabolic labeling of platelets is fairly easy to perform and can be easily integrated into existing platelet transfusion protocols by simply adding azido-sugars to the platelet storage media [39,40]. Our platelet labeling and targeting approach enables *ex vivo* conjugation of various types of cargos to platelets and *in vivo* conjugation of cargos to adoptively transferred platelets.

We also explored the feasibility of metabolically label platelets *in vivo* via i.p. injection of azido-sugars. Azido-sugars managed to label platelets in the bloodstream with azido groups, and the azido tags remain on platelet membrane for up to 4 days, nearly the lifespan of mouse platelets (3–5 days). Platelets from azido-sugar-treated mice and control mice exhibited negligible differences in counts, viability, and activation status, supporting the benign safety profile of azido-sugar towards platelets. The ability to metabolically tag circulating platelets with azido groups *in vivo* opens up new opportunities for targeted delivery of diagnostic and therapeutic agents to platelets and the orchestration of interactions between circulating platelets and other cells. For example, immunomodulatory agents such as checkpoint blockades and cytokines can be attached to platelets *in vivo* for subsequent trafficking to tumors for potentially enhanced therapeutic efficacy. Anti-inflammatory agents can be delivered to wounded tissues and other disease sites via platelets to facilitate the resolution of inflammation and restoration of diseased tissues. We also envision the potential attachment of hemostatic agents to platelets via the *in vivo* platelet labeling and targeting technology for the prevention of internal bleeding in tissues.

To conclude, we report the successful metabolic glycan labeling of anucleate platelets *in vitro* and *in vivo*. Ac₄ManAz can metabolically label platelets with azido groups in a concentration and incubation time dependent manner, with cell-surface azido groups detectable at as early as 4 h. Azido-labeled platelets can covalently capture various types of molecules via efficient click chemistry, including proteins, polymers, and small-molecule drugs. Drugs, upon conjugation to azido-labeled platelets, can be gradually released to effect on neighboring cancer

cells. We further demonstrate that intraperitoneally injected Ac₄ManAz can label circulating platelets with azido groups *in vivo*. This *in vitro* and *in vivo* platelet labeling and targeting technology opens a new avenue to a variety of platelet-based therapeutic applications. Our study also expands the applicability of the metabolic glycan labeling technology to platelets and other cells alike that are non-proliferative, nucleus-free, and lacking efficient protein machinery.

4. Online methods

Materials and Instrumentation. D-Mannosamine hydrochloride, D-galactoseamine hydrochloride, D-glucosamine hydrochloride, Doxorubicin Hydrochloride, DBCO-Cy5, Poly(acrylic acid) (2 kDa), sodium azide, chloroacetic anhydride, acetic anhydride, MTT, Collagen and other chemical reagents were purchased from Sigma Aldrich (St. Louis, MO, USA) unless otherwise noted. DBCO-Cy5 and DBCO-sulfo-amine were purchased from Vector Lab (Newark, CA, USA). eFlour 780 fixable viability dye (65-0865-14), CD41-FITC (11-0411-82), CD62p-PE (12-0626-82), Calcein AM (C1430), AnnexinV-APC (A35110), Polylsine (A3890401), Anti-APC biotin (13-4170-82) and Avidin-FITC (A821) were obtained from Thermo Fisher (Ashville, NC, USA). Prostaglandin E1 was purchased from MedChemExpress (Monmouth Junction, NJ, USA). Allophycocyanin and Phycoerythrin were purchased from AAT Bioquest (Pleasanton, CA, USA). N-hydroxysuccinimide (NHS) and 3-(3-Dimethylaminopropyl)-1-ethyl-carbodiimide hydrochloride (EDC) were purchased from Chem-Impex (Wood Dale, IL, USA). TMRE was purchased from Cell Signaling Technology. Annexin V binding buffer (10x) was obtained from BD Biosciences. High-performance liquid chromatography (HPLC) analysis was performed on a Shimadzu CBM-20A system (Shimadzu, Kyoto, Japan) equipped with an SPD-20A PDA detector (190–800 nm), an RF-20A fluorescence detector, and an analytical C18 column (Shimadzu, 3 μ m, 50 \times 4.6 mm, Kyoto, Japan). Preparative HPLC was performed on a CombiFlash®Rf system (Teledyne ISCO, Lincoln, NE, USA) equipped with a RediSep®Rf HP C18 column (Teledyne ISCO, 30 g, Lincoln, NE, USA). Lyophilization was conducted

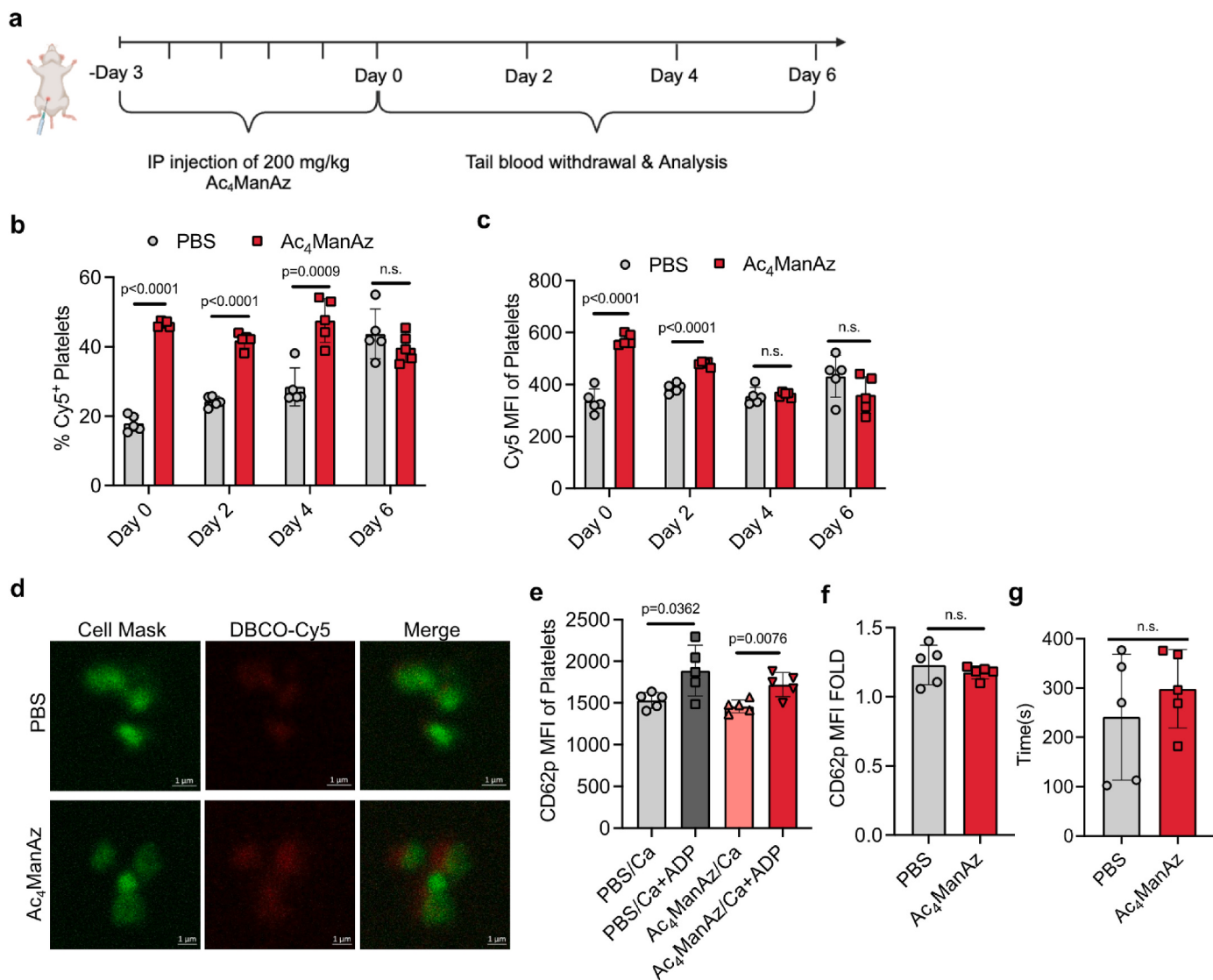


Fig. 5. In vivo metabolic labeling of platelets. (a) Timeframe of *in vivo* labeling study. Ac₄ManAz was i.p. injected twice a day for three days. Blood was drawn at 6 h, 2 days, 4 days, and 6 days for the isolation of platelets. Platelets were incubated with DBCO-Cy5 to detect surface azido groups. (b) % Cy5⁺ platelets harvested at different times and stained with DBCO-Cy5 (n = 5). (c) Mean Cy5 fluorescence intensity of platelets harvested at different times and stained with DBCO-Cy5 (n = 5). (d) Confocal images of platelets isolated from Ac₄ManAz- or PBS-treated mice on day 2 and stained with DBCO-Cy5. (e) CD62p expression levels of platelets after stimulation with Ca²⁺ and ADP or Ca²⁺ only (n = 5). Platelets were harvested on day 2. (f) Fold-increase of CD62p levels after stimulation with Ca²⁺ and ADP or Ca²⁺ only (n = 5). Platelets were harvested on day 2. (g) Time till the cessation of bleeding, as determined via the tail bleed assay (n = 5). All the numerical data are presented as mean ± SD (two tailed unpaired student's t-test was used; n.s., P > 0.05; 0.01 < *P ≤ 0.05; **P ≤ 0.01; ***P ≤ 0.001; ****P ≤ 0.0001).

in a Labconco FreeZone lyophilizer (Kansas City, MO, USA). Nuclear Magnetic Resonance (NMR) spectra were recorded on a Varian U500 (500 MHz) or VXR500 (500 MHz), or a Bruker Carver B500 (500 MHz) spectrometer. Electrospray ionization (ESI) mass spectra were obtained from a Waters ZMD Quadrupole Instrument (Waters, Milford, MA, USA). Confocal laser scanning microscopy (CLSM) images were taken by using a Zeiss LSM 700 or LSM 880 Confocal Microscope (Carl Zeiss, Thornwood, NY, USA). Western blotting protein bands were imaged on an ImageQuant LAS 4010 gel imaging system (GE, Pittsburgh, PA, USA). Flow cytometry analysis was conducted on an Attune NxT flow cytometer and analyzed on FlowJo V10.8.1. Matrix-Assisted Laser Desorption Ionization (MALDI) was obtained from Bruker Daltonics UltraflexXtreme MALDI TOF.

Cell line and animals. C1498 AML cell line was purchased from the American Type Culture Collection (Manassas, VA, USA). C1498 cells were cultured in DMEM/F12 media containing 10 % bovine calf serum (Gibco), 100 units/mL Penicillin G and 100 µg/mL streptomycin

(Invitrogen, Carlsbad, CA, USA) at 37 °C in 5 % CO₂ humidified incubator. Female C57BL/6 mice were purchased from the Jackson Laboratory (Bar Harbor, ME, USA). Feed and water were available ad libitum. Artificial light was provided in a 12 h/12 h cycle. All procedures involving animals were done in compliance with the National Institutes of Health and Institutional guidelines with approval from the Institutional Animal Care and Use Committee at the University of Illinois at Urbana-Champaign.

Platelet isolation. Retro orbital blood extraction was used to extract blood, the blood was immediately transferred into the Acid-Citrate Dextrose Buffer (85 mmol/L trisodium citrate, 71 mmol/L citric acid, and 111 mmol/L dextrose). Modified Tyrodes Calcium free buffer with 1 % EGTA was added to the blood and pipetted carefully. The tubes containing blood were then spun at 200 rcf to remove the red blood cells. The supernatant was extracted carefully. Another centrifugation step at 500 rcf was performed to remove any remaining red blood cells or lymphocytes. The supernatant was transferred to the resuspension

buffer containing 0.5 μ M ProstaglandinE-1 (PGE-1). The solution was then spun at 1200 rcf to pellet the platelets. The platelets were then resuspended in the resuspension buffer containing PGE-1.

Platelet buffer and temperature comparison. Alsever's solution (MP Biomedicals) was supplemented with 0.2 % (w/v) BSA. The composition of Platelet buffer 1 (PB1) is a Modified Tyrodes Calcium Free buffer consisting of 80.4 mM NaCl, 1.8 mM KCl, 0.18 mM NaH₂PO₄, 1.2 mM MgCl₂, 3 mM HEPES, 3 mM glucose, 0.53M NaHCO₃, 1.2 % BSA. Platelet buffer 2 (PLT2) is also a Modified Tyrodes Calcium Free Buffer consisting of 134 mM NaCl, 3 mM KCl, 0.3 mM NaH₂PO₄, 2 mM MgCl₂, 5 mM HEPES, 5 mM glucose, 12 mM NaHCO₃, 0.2 % BSA. Platelets were incubated in different buffers for 24 h at 4 °C, 24 °C and 37 °C, respectively. Cells were then stained with FITC-conjugated anti-CD41 and eflour 780 fixable viability dye for 20 min at room temperature and then washed twice, prior to flow cytometry analysis.

Synthesis of Ac₄ManAz, Ac₄GalAz, and Ac₄GluAz. [30,31] To a solution of D-mannosamine hydrochloride or D-galactosamine hydrochloride or D-glucosamine hydrochloride (1.00 g, 4.64 mmol) in methanol (10 mL) was dropwise added 0.5 N sodium methoxide in methanol (9.3 mL, 4.64 mmol) at 0°C. The mixture was stirred at room temperature for 30 min. Triethylamine (0.47 g, 4.64 mmol) and chloroacetic anhydride (0.95 g, 5.57 mmol, 95 %) were then added. The reaction mixture was stirred overnight, followed by the addition of H₂O (3 mL) and sodium azide (1.21g, 18.56 mmol). After stirred overnight at 65 °C, the precipitate was filtered out and the filtrate was concentrated. The residue was suspended in pyridine (15 mL), followed by the addition of 4-dimethylaminopyridine (56.8 mg, 0.47 mmol) and acetic anhydride (3.79 g, 37.12 mmol). The mixture was stirred overnight at room temperature, and then quenched with methanol. After the removal of solvents, the residue was dissolved in ethyl acetate and washed successively with HCl (1 M), brine, and saturated NaHCO₃ (aq). The organic layer was dried over Na₂SO₄ and filtered. The filtrate was concentrated, and the crude product was purified by silica gel column chromatography to yield a white foam (1.40 g, 70 % yield). LRMS (ESI) *m/z*: calculated for Ac₄ManAz C₁₆H₂₂N₄O₁₀Na [M+Na]⁺ 453.1, found 453.1. ¹H NMR of Ac₄ManAz (CDCl₃, 500 MHz): δ (ppm) 6.66&6.60 (d, *J* = 9.0 Hz, 1H, C(O)NHCH), 6.04&6.04 (d, 1H, *J* = 1.9 Hz, NHCHCHO), 5.32–5.35&5.04–5.07 (dd, *J* = 10.2, 4.2 Hz, 1H, CH₂CHCHCH), 5.22&5.16 (t, *J* = 9.9 Hz, 1H, CH₂CHCHCH), 4.60–4.63&4.71–4.74 (m, 1H, NHCHCHO), 4.10–4.27 (m, 2H, CH₂CHCHCH), 4.07 (m, 2H, C(O)CH₂N₃), 3.80–4.04 (m, 1H, CH₂CHCHCH), 2.00–2.18 (s, 12H, CH₃C(O)). ¹³C NMR of Ac₄ManAz (CDCl₃, 500 MHz): δ (ppm) 170.7, 170.4, 170.3, 169.8, 168.6, 168.3, 167.5, 166.9, 91.5, 90.5, 73.6, 71.7, 70.5, 69.1, 65.3, 65.1, 62.0, 61.9, 52.8, 52.6, 49.9, 49.5, 21.1, 21.0, 21.0, 20.9, 20.9, 20.9, 20.8.

Platelet labeling. Following platelet isolation, Ac₄ManAz (or Ac₄GalAz or Ac₄GluAz) was added to the medium at concentrations ranging from 25 μ M to 400 μ M. The platelets were stored at room temperature for 4 h on a shaker at an RPM of 90. Platelets were washed twice to remove the sugar and then incubated with DBCO-Cy5 for 1 h at room temperature. Cells were then washed and incubated with FITC-conjugated anti-CD41 and eflour 780 fixable viability dye for 20 min at room temperature. The platelets were then washed twice and suspended in 0.4 % PFA for flow cytometry analysis. For some experiments, platelets were incubated with azido-sugars for an extended time (24 or 48 or 72 h).

Western Blot analysis of platelets. Platelets were treated with 200 μ M Ac₄ManAz or PBS for 4 h, washed twice, and transferred to a lysis buffer (50 mM Tris-HCl, 1 % SDS, pH 7.4). The buffer was sonicated and centrifuged at 2000 rcf and then at 21,000 rcf to yield the protein pellet. The protein was quantified with a BCA assay and diluted accordingly. This was followed by blocking with iodoacetamide for an hour at 37 °C. Laemmli buffer was then added to the solution prior to performing the gel electrophoresis on a 4–20 % gel (MiniPROTEAN TGX precast gel, Bio-Rad). Protein bands were then transferred to a nitrocellulose membrane. The membrane was blocked with BSA for overnight, washed,

and stained with DBCO-biotin for 1 h at room temperature, followed by streptavidin-HRP staining and chemiluminescence imaging.

Platelet viability and necrosis. Platelets were collected and incubated with 100 μ M Ac₄ManAz or PBS for 10 min, 24 h, 48 h, and 72 h, respectively. Platelets were then washed twice and stained with TMRE in PBS for 30 min at room temperature. After staining, platelets were washed twice and analyzed with a flow cytometer. To study necrosis, platelets were transferred to an annexin binding buffer and stained with Annexin-APC and Calcein AM for 30 min at room temperature. The platelets were washed once using the binding buffer and then analyzed on a flow cytometer.

Azido retention on platelets. Platelets were collected on the same day and incubated with 100 μ M Ac₄ManAz for 24 h. Platelets were washed twice, resuspended in the resuspension medium for varied time, and stained with DBCO-Cy5 for 1 h. Platelets were also stained with FITC-conjugated anti-CD41 and eflour 780 fixable viability dye for 20 min at room temperature. Cells were washed twice and resuspended in 0.4 % PFA prior to flow cytometer analysis.

Collagen aggregation assay. Glass slides were first coated with polylysine. Collagen was dissolved in 0.01 M HCl at a concentration of 1 mg/mL, stirred for 3 h, diluted to a concentration of 50 μ g/mL using 0.01 M HCl, and then poured onto polylysine-coated slides. After 1 h, the slides were washed twice with PBS and then dried for use. Platelets were added with 2.5 mM CaCl₂ prior to placement onto the collagen-coated slides. Platelets with calcium were also placed on slides without collagen coating as the control. The slides were imaged 10 min after the addition of platelets.

DBCO modification of proteins. Allophycocyanin (APC) or Phycoerythrin (PE) (2 mg/mL) was mixed with DBCO-sulfo-NHS (40-fold in molar concentration). The mixture was stirred at room temperature in the dark for 1 h, and washed 5 times to remove unreacted DBCO-sulfo-NHS using Amicon ultracentrifugation filters (3 kDa). To confirm conjugation, UV-vis spectra of DBCO-modified proteins and unmodified proteins were taken.

Protein conjugation to platelets. Platelets were incubated with 100 μ M Ac₄ManAz or PBS at room temperature for 24 h. After washing, platelets were incubated with DBCO-modified or unmodified proteins (APC or PE, 0.05 mg/mL) for 1 h. Platelets were then incubated with FITC-conjugated anti-CD41 and eflour 780 fixable viability dye for 20 min at room temperature, washed twice, and suspended in 0.4 % PFA prior to flow cytometer analysis. For confocal imaging, platelets pre-incubated with DBCO-APC and FITC-conjugated anti-CD41 were fixed with 4 % PFA for 30 min. Platelets were then centrifuged at 1200 rcf and re-suspended in PBS. One droplet of platelets was added onto a microscope slide, added Prolong Gold, and covered with a coverslip. Imaging was performed on a Zeiss LSM 700.

APC retention assay. Platelets were incubated with 100 μ M Ac₄ManAz or PBS at room temperature. After 24 h, platelets were washed and stained with DBCO-APC. Platelets were then washed and resuspended in resuspension media till analysis. All groups were analyzed together by first staining with biotin-conjugated anti-APC for 30 min. Platelets were washed twice and then stained with Avidin-FITC and eflour 780 fixable viability dye for 15 min. Platelets were washed twice and then suspended in 0.4 % PFA prior to flow cytometer analysis.

Synthesis of DBCO-PAA and DBCO/Cy5-PAA. PAA (2 kDa, 10 mg) was dissolved in DMSO and mixed with NHS (18 mg) and EDC (200 mg) with vigorous stirring for overnight. The solution was dialyzed against deionized water for 48 h. The polymer was then lyophilized and NMR spectra were collected to confirm DBCO conjugation. For DBCO/Cy5-PAA synthesis, DBCO-PAA and Cy5-azide were dissolved in DMSO and stirred for 24 h at room temperature. Polymers were then precipitated in dichloromethane, washed with water, and lyophilized for use.

DBCO-PAA conjugation to platelets. Platelets were incubated with 100 μ M Ac₄ManAz or PBS for 24 h, and then incubated with 0.01 mg/mL of DBCO-PAA or PAA for 1 h at room temperature. Platelets were then stained with FITC-conjugated anti-CD41 and eflour 780 fixable viability

dye for 20 min at room temperature, washed twice, and suspended in 0.4 % PFA prior to flow cytometer analysis.

DBCO-hz-Dox synthesis. DBCO-NHS (30 mg) and DIPEA (20 μ L) were dissolved in acetonitrile (100 mL), followed by the addition of hydrazine monohydrate (45 μ L). After 30 min, acetonitrile was removed using the rotavapor. The DBCO-hydrazide film was dissolved in methanol, followed by the addition of doxorubicin in methanol and trifluoroacetic acid (200 μ L). The mixture was stirred overnight, followed by purification using a preparative HPLC. LRMS (ESI) *m/z*: exact mass calculated for C₄₆H₄₅N₄O₁₂ [M+H]⁺ 845.3, found 845.6.

DBCO-hz-Dox conjugation to platelets. Platelets were incubated with 100 μ M Ac₄ManAz or PBS for 24 h, and then incubated with 10 μ M DBCO-hz-DOX for 1 h at room temperature. Platelets were then stained with FITC-conjugated anti-CD41 and fixable viability dye eflour 780 for 20 min at room temperature, washed twice, and suspended in 0.4 % PFA prior to flow cytometer analysis.

DBCO-hz-dox degradation and dox release. DBCO-hz-Dox degradation was tested in a Sodium Citrate Buffer of pH 5.4 or PBS buffer of pH 7.4. DBCO-hz-Dox was incubated in the buffers, and aliquots of solution were run on the HPLC (under fluorescence mode) at different times, with the ratio of Dox to DBCO-Dox calculated based on the standard curves of free Dox and DBCO-Dox.

Platelet-C1498 AML cocultures. Platelets were incubated with 100 μ M Ac₄ManAz or PBS for 24 h, and then incubated with DBCO-hz-Dox (1 μ M, 10 μ M, or 100 μ M) for 1 h at room temperature. Platelets and C1498 AML cells were then seeded into 96-well plates (10,000 AML cells and 30,000 platelets per well). After 48 h, cells were spun down at 300 rcf to selectively pellet the AML cells. MTT assay of AML cells was then performed to assess the viability.

In vivo labeling of platelets. C57BL/6 mice were intraperitoneally injected with Ac₄ManAz (200 mg/kg) or PBS every 12 h over 3 days. Blood was obtained from the tail vein at 6 h, 2 days, 4 days, 6 days, and 8 days, respectively post injections of Ac₄ManAz or PBS, and collected into tubes containing ACD buffer. Platelets were then extracted following the platelet isolation protocol. Platelets were then incubated with 5 μ M DBCO-Cy5 for 1 h and then stained with FITC-conjugated anti-CD41 and eflour 780 fixable viability dye for 20 min at room temperature, washed twice, and suspended in 0.4 % PFA prior to flow cytometer analysis. For confocal imaging, one droplet of platelets was added onto a microscope slide, added Prolong Gold, and covered with a coverslip. Imaging was performed on Zeiss LSM 700.

Platelet CD62p level analysis. In-vivo labeled platelets were isolated as previously described. 2.5 mM Ca²⁺ was added to the platelets, which were then incubated with 10 μ M Adenosine diphosphate for 30 min. Cells were then washed and stained with FITC-conjugated anti-CD41, PE-conjugated anti-CD62p, and eflour 780 fixable viability dye for 20 min at room temperature. Cells were then washed twice and suspended in 0.4 % PFA for flow cytometry analysis.

Tail bleed assay. C57BL/6 mice were intraperitoneally injected with Ac₄ManAz (200 mg/kg) or PBS every 12 h over 3 days. Mice were injected with carprofen (5 mg/kg), anesthetized under isoflurane, and marked on the tail at 10 mm from the tail tip. The tail was then amputated using a sharp scalpel. The bleeding was monitored till cessation, with the time of complete bleed stoppage noted.

Statistical analysis. Statistical analysis was performed using GraphPad Prism v6 and v8. Sample variance was tested using the F test. For two-group comparisons, the two-tailed unpaired student's t-test was used. For multiple-group comparisons, a one-way analysis of variance (ANOVA) with post hoc Tukey's LSD test was used.

CRediT authorship contribution statement

Dhyanesh Baskaran: Writing – review & editing, Writing – original draft, Methodology, Investigation, Formal analysis, Conceptualization. **Yusheng Liu:** Writing – review & editing, Investigation. **Jiadiao Zhou:** Writing – review & editing, Investigation. **Yueji Wang:** Writing – review

& editing, Investigation. **Daniel Nguyen:** Writing – review & editing, Investigation. **Hua Wang:** Writing – review & editing, Supervision, Project administration, Funding acquisition, Conceptualization.

Declaration of competing interest

The authors declare that they have no known competing financial interests or personal relationships that could have appeared to influence the work reported in this paper.

Acknowledgements

The authors would like to acknowledge the financial support from NSF DMR 2143673 CAR, NIH R01CA274738, NIH R21CA270872, and the start-up package from the Department of Materials Science and Engineering at the University of Illinois at Urbana-Champaign and the Cancer Center at Illinois. Research reported in this publication was supported by the Cancer Scholars for Translational and Applied Research (C^{*}STAR) Program sponsored by the Cancer Center at Illinois and the Carle Cancer Center under Award Number CST EP012023.

Appendix A. Supplementary data

Supplementary data to this article can be found online at <https://doi.org/10.1016/j.mtbiol.2025.101719>.

Data availability

Data will be made available on request.

References

- [1] M.E. Quach, W. Chen, R. Li, Mechanisms of platelet clearance and translation to improve platelet storage. <http://ashpublications.org/blood/article-pdf/131/14/1512/1405604/blood743229.pdf>, 2018.
- [2] K.D. Mason, et al., Programmed anuclear cell death delimits platelet life span, *Cell* 128 (2007) 1173–1186.
- [3] P.E.J. van der Meijden, J.W.M. Heemskerk, Platelet biology and functions: new concepts and clinical perspectives, *Nat. Rev. Cardiol.* 16 (2019) 166–179, <https://doi.org/10.1038/s41569-018-0110-0>. Preprint at.
- [4] A.M. Behrens, M.J. Sikorski, P. Kofinas, Hemostatic strategies for traumatic and surgical bleeding, *J. Biomed. Mater. Res.* 102 (2014) 4182–4194.
- [5] M. Tomaiuolo, L.F. Brass, T.J. Stalker, Regulation of platelet activation and coagulation and its role in vascular injury and arterial thrombosis, *Interventional Cardiology Clinics* 6 (2017) 1–12, <https://doi.org/10.1016/j.jiccl.2016.08.001>. Preprint at.
- [6] S.H. Yun, E.H. Sim, R.Y. Goh, J.I. Park, J.Y. Han, Platelet activation: the mechanisms and potential biomarkers, *BioMed Res. Int.* 2016 (2016), <https://doi.org/10.1155/2016/9060143>. Preprint at.
- [7] L. Nicolai, K. Pekayaz, S. Massberg, Platelets: orchestrators of immunity in host defense and beyond, *Immunity* 57 (2024) 957–972, <https://doi.org/10.1016/j.immuni.2024.04.008>. Preprint at.
- [8] M. Mir, et al., Synthetic polymeric biomaterials for wound healing: a review, *Progress in Biomaterials* 7 (2018), <https://doi.org/10.1007/s40204-018-0083-4>. Preprint at.
- [9] O. Yakovenko, et al., Serine-rich repeat adhesins mediate shear-enhanced streptococcal binding to platelets, *Infect. Immun.* 86 (2018).
- [10] C. Chaipan, et al., DC-SIGN and CLEC-2 mediate human immunodeficiency virus type 1 capture by platelets, *J. Virol.* 80 (2006) 8951–8960.
- [11] J.P. Stone, D.D. Wagner, P-selectin mediates adhesion of platelets to neuroblastoma and small cell lung cancer, *J. Clin. Investig.* 92 (1993) 804–813.
- [12] C. Hinterleitner, et al., Platelet PD-L1 reflects collective intratumoral PD-L1 expression and predicts immunotherapy response in non-small cell lung cancer, *Nat. Commun.* 12 (2021).
- [13] J. Leung, M.F. Cau, C.J. Kastrup, Emerging gene therapies for enhancing the hemostatic potential of platelets, *Transfusion (Paris)* 61 (2021).
- [14] T. Thijss, H. Deckmyn, K. Broos, Model systems of genetically modified platelets, *Blood, The Journal of the American Society of Hematology* 119 (2012) 1634–1642.
- [15] C. Figueiredo, R. Blasczyk, Generation of HLA universal megakaryocytes and platelets by genetic engineering, *Front. Immunol.* 12 (2021) 768458.
- [16] N. Zhang, et al., CRISPR/Cas9-mediated conversion of human platelet alloantigen allotypes, *Blood, The Journal of the American Society of Hematology* 127 (2016) 675–680.
- [17] Q. Shi, Platelet-targeted gene therapy for hemophilia, *Molecular Therapy Methods & Clinical Development* 9 (2018) 100–108.

- [18] S. Novakowski, K. Jiang, G. Prakash, C. Kastrup, Delivery of mRNA to platelets using lipid nanoparticles, *Sci. Rep.* 9 (2019).
- [19] J. Li, C.C. Sharkey, B. Wun, J.L. Liesveld, M.R. King, Genetic engineering of platelets to neutralize circulating tumor cells, *J. Contr. Release* 228 (2016) 38–47.
- [20] A.S. Weyrich, et al., Change in protein phenotype without a nucleus: translational control in platelets, *Semin. Thromb. Hemost.* 30 (2004) 491–498.
- [21] C. Strong, et al., Genetic engineering of transfusible platelets with mRNA-lipid nanoparticles is compatible with blood banking practices, *Blood* 144 (2024) 2223–2236.
- [22] J. Leung, et al., Genetically engineered transfusible platelets using mRNA lipid nanoparticles, *Sci. Adv.* 9 (2023) eadi0508.
- [23] C. Wang, et al., In situ activation of platelets with checkpoint inhibitors for post-surgical cancer immunotherapy, *Nat. Biomed. Eng.* 1 (2017).
- [24] Y. Wang, et al., Active recruitment of anti-PD-1-conjugated platelets through tumor-selective thrombosis for enhanced anticancer immunotherapy. <http://www.science.org>, 2023.
- [25] L. Dai, N. Gu, B.-A. Chen, G. Marriott, Human platelets repurposed as vehicles for *in vivo* imaging of myeloma xenotransplants, *Oncotarget* 7 (2016) 21076–21090.
- [26] J.D. Hohmann, et al., Delayed targeting of CD39 to activated platelet GPIIb/IIIa via a single-chain antibody: breaking the link between antithrombotic potency and bleeding? *Blood*, The Journal of the American Society of Hematology 121 (2013) 3067–3075.
- [27] M.-J. Jacobin-Valat, et al., Nanoparticles functionalised with an anti-platelet human antibody for *in vivo* detection of atherosclerotic plaque by magnetic resonance imaging, *Nanomed. Nanotechnol. Biol. Med.* 11 (2015) 927–937.
- [28] Rivera, J., Lozano, M. L. & Vicente, V. In vitro changes of platelet parameters: lessons from blood banking. in *Platelets and Megakaryocytes* 057–072 (Humana Press, New Jersey). doi:10.1385/1-59259-783-1:057.
- [29] H.M. Rinder, et al., Progressive platelet activation with storage: evidence for shortened survival of activated platelets after transfusion, *Transfusion (Paris)* 31 (1991) 409–414.
- [30] H. Wang, D.J. Mooney, Metabolic glycan labelling for cancer-targeted therapy, *Nat. Chem.* 12 (2020) 1102–1114, <https://doi.org/10.1038/s41557-020-00587-w>. Preprint at.
- [31] H. Wang, et al., Selective *in vivo* metabolic cell-labeling-mediated cancer targeting, *Nat. Chem. Biol.* 13 (2017) 415–424.
- [32] P.R. Wratil, R. Horstkorte, W. Reutter, Metabolisches Glykoengineering mit N-Acyl-Seiten-ketten-modifizierten Mannosaminen, *Angew. Chem.* 128 (2016) 9632–9665.
- [33] F. Jóhannsson, et al., Systems analysis of metabolism in platelet concentrates during storage in platelet additive solution, *Biochem. J.* 475 (2018) 2225–2240.
- [34] J. Im, R. Muschel, Protocol for murine/mouse platelets isolation and their reintroduction *in vivo*, *Bio Protoc* 7 (2017).
- [35] L. Lian, et al., Loss of pleckstrin defines a novel pathway for PKC-mediated exocytosis, *Blood* 113 (2009) 3577–3584.
- [36] C. Aubron, A.W.J. Flint, Y. Ozier, Z. McQuilten, Platelet storage duration and its clinical and transfusion outcomes: a systematic review, *Crit. Care* 22 (2018), <https://doi.org/10.1186/s13054-018-2114-x>. Preprint at.
- [37] T. Ozpolat, et al., Evaluating stored platelet shape change using imaging flow cytometry, *Platelets* 34 (2023).
- [38] V. Rumjantseva, K.M. Hoffmeister, Novel and unexpected clearance mechanisms for cold platelets, *Transfus. Apher. Sci.* 42 (2010) 63–70.
- [39] M. Stolla, et al., Platelet transfusion â“ the new immunology of an old therapy, *Front. Immunol.* 6 (2015).
- [40] J. Sahler, et al., Platelet storage and transfusions: new concerns associated with an old therapy, *Drug Discov. Today Dis. Mech.* 8 (2011) e9–e14.